JAAS

Accepted Manuscript

This is an *Accepted Manuscript*, which has been through the Royal Society of Chemistry peer review process and has been accepted for publication.

Accepted Manuscripts are published online shortly after acceptance, before technical editing, formatting and proof reading. Using this free service, authors can make their results available to the community, in citable form, before we publish the edited article. We will replace this *Accepted Manuscript* with the edited and formatted *Advance Article* as soon as it is available.

You can find more information about *Accepted Manuscripts* in the Information for Authors.

Please note that technical editing may introduce minor changes to the text and/or graphics, which may alter content. The journal's standard Terms & Conditions and the Ethical guidelines still apply. In no event shall the Royal Society of Chemistry be held responsible for any errors or omissions in this *Accepted Manuscript* or any consequences arising from the use of any information it contains.

ROYAL SOCIETY OF CHEMISTRY

www.rsc.org/jaas

Journal Name

RSCPublishing

ARTICLE

Detection characteristics of iodine by low pressure and short pulse laser-induced breakdown spectroscopy (LIBS)

Xiaobo Zhang, [a b] Yoshihiro Deguchi,*[b] Zhenzhen Wang, [a b] Junjie Yan [a] and Jiping Liu [a]

Cite this: DOI: 10.1039/xoxxoooooox

Received ooth January 2012,
Accepted ooth January 2012

DOI: 10.1039/xoxxoooooox

www.rsc.org/

In this study, Laser-Induced Breakdown Spectroscopy (LIBS) technology has been applied to detect iodine, an essential element for human body. Iodine in buffer gases of N_2 and air was detected using nanosecond and picosecond breakdowns of CH_3I at reduced pressure. Compared with the conventional methods of iodine measurement, LIBS technology without the sample preparation shows the merits of fast response, real-time and enhanced detection limit. The measurement results of iodine demonstrated that low-pressure LIBS is the favourable method for trace species measurement in analytical application. The plasma generation process can be controlled by the pressure and laser pulse width for the larger ionization and excitation processes of iodine, which was discussed by the intensity ratio of iodine emission at 183 nm to nitrogen emission at 174.3 nm. The detection limit of iodine measurement in N_2 was 60 ppb in nanosecond breakdown at 700 Pa. Iodine in the buffer gas of air was also detected using nanosecond and picosecond breakdowns to discuss the effect of oxygen.

Introduction

Iodine is a necessary element in the environment, contained in most materials, such as soil, rocks, ocean, food, and so on. Iodine is also one of the essential trace elements of the human body, called intellectual element. The total amount of iodine in healthy adult is about 20-50 mg, 70%-80% of which exist in the thyroid gland. The World Health Organization (WHO) recommends the intake of iodine should not exceed 300 μg a day. Nuclear accidents show that the radioactive iodine is the serious influencing factor for human health and environment. For example, in Japan, after the Fukushima nuclear power plant accident, the pollution of the radioactive materials becomes the focal issue and research point. Human and other organisms can take in the radioactive materials, such as iodine, Cs, Sr, Se and so on, which leads to severe disease.

There are several papers proposing various methods for iodine detection in food, brine, air, etc. The technology of Gas Chromatography-Mass Spectrometry (GC-MS) was employed to determinate iodine in various applications.[1, 2] The high mobility of iodine in aquatic systems has led to ^{129}I contamination problems at sites where nuclear fuel has been reprocessed. In order to assess the distribution of ^{129}I and stable ^{127}I in environmental systems, a sensitive and rapid method was developed which enables determination of isotopic ratios of iodine. Iodide concentrations were quantified using Gas Chromatography-Mass Spectrometry (GC-MS).[3] A new approach of the combination with post derivatization and Gas Chromatography-Mass Spectrometry (GC-MS) for the quantification of gaseous molecular iodine (I_2) was presented for laboratory- and field-based studies and its novel application for the measurement of radioactive molecular iodine.[4] Inductively Coupled Plasma associated with Optical Emission Spectroscopy (ICP-OES) and Mass Spectrometry (ICP-MS) technologies have been successfully applied to analyze iodine in different kinds of samples.[5-7] Several sample preparation techniques have been evaluated for the determination of iodine using UV-photochemical generation-quadrupole inductively coupled plasma mass spectrometry, which was applied to the analysis of real samples.[8] However, sample preparation was required to utilize these technologies.

Laser-Induced Breakdown Spectroscopy (LIBS) is an appealing detection technique compared with many other methods of elemental analysis because of the fast response, high sensitivity, real-time and non-contact features without any pre-preparation of samples. The technology has been widely used in gas,[9-15] liquid[16-18] and solid materials.[19-24] With the development of the laser technology, short pulse width lasers, such as picosecond laser and femtosecond laser have been employed for LIBS technique. The utilization of short pulse laser for plasma generation has been extensively studied.[25, 26] Short pulse irradiation allowed for a specificity of excitation that could yield LIBS signals more tightly and showed significantly lower background emission.

Laser-induced plasma process in gas phase is different from that in solid phase. One of the challenging targets of LIBS is the enhancement of detection limit of gas phase materials. In this paper, iodine in buffer gases of N_2 and air was detected by LIBS technology using nanosecond and picosecond breakdowns of CH_3I at reduced pressure. The laser-induced plasma process such as the electron impact ionization process can be controlled by reducing the pressure and employing short pulse laser. The method reported here can improve the detection ability of iodine measurement in practical applications.

Theory

Creation and cooling processes of plasma in LIBS can be described as follows. In the generation of plasma, the core of plasma is firstly produced by the absorption of the incident laser energy, such as multi-photon ionization in solids, liquids, or gases. The creation of the plasma core induces the rapid growth of plasma through the absorption of the laser light by electrons and the electron impact ionization process in it, that is, the inverse bremsstrahlung process. After the termination of the laser pulse, the plasma continues expanding because of its high temperature and pressure gradients compared with ambient conditions. At the same time, recombination of electrons and ions proceeds due to the collision process and temperature decreases gradually compared with the plasma generation process. Therefore the continuum emission is released by bremsstrahlung and recombination processes in the optically thin plasma. LIBS signals of ions, atoms and molecules arise in the plasma cooling period.[27] The continuum emission is considered as one of the interferences to LIBS signals.

Despite the fact that the processes involved in LIBS are complex, the emission intensity from the optically thin plasma during the cooling process was mostly examined by the following equation with the assumption of a uniform plasma temperature and no self-absorption:[27]

$$I_{(i)} = n_{(i)} \sum_j \left\{ K_{(i),j} g_{(i),j} \exp\left(-\frac{E_{(i),j}}{k_B T} \right) \right\} \quad (1)$$

In the above expression, $I_{(i)}$ is the emission intensity of species i, $n_{(i)}$ is the concentration of species i, $K_{(i),j}$ is a variable that includes the Einstein A coefficient from the upper energy level j, $g_{(i),j}$ is the statistical weight of species i at the upper energy level j, $E_{(i),j}$ is the upper level energy of species i, k_B is the Boltzmann constant and T is the plasma temperature. Eq. (1) is applicable under the conditions of local thermodynamic equilibrium (LTE).

There are several interferences with the target signals in LIBS process, generally including the continuum emission from plasma itself, coexisting molecular and atomic emissions, noise from detectors, and so on. At high pressure, the main interference is the continuum emission from plasma itself, the intensity of which is proportional to biquadratic temperature. The plasma temperature including the temperatures of electrons, ions and neutrals is also high. The generated plasma is dense and the electrons, ions and neutrals collide frequently with each other. The temperatures of electrons, ions and neutrals become approximately same through violent collision to transfer energy in high pressure plasma, generally called thermal plasma. At low pressure, however, the density of plasma is rather low and few opportunities of the collisions between electrons and other particles cause the large difference of kinetic energy. Once initial electrons and ions are produced, they are accelerated by absorbing laser energy intensely. Because of the mass difference between charged particles, the kinetic energy of electron is much higher. Since the neutrals obtain the energy by the collision of particles, the kinetic energy of neutrals is lower compared with that of the charged particles. In this case these particles are not in local thermodynamic equilibrium (LTE) condition. T_e, T_i and T_n are defined as the kinetic temperatures of electrons, ions and neutrals respectively and the temperatures are in the order $T_e >> T_i$, $T_e >> T_n$, which is called cold plasma. In this case, the departure from LTE produces a population of excited levels differing from Boltzmann distribution. Populations of ions and neutrals in upper energy levels are larger than that of the LTE condition.[28] This phenomenon becomes eminent in the low pressure condition in which collisions are reduced and the expansion of plasma becomes faster. The interference of coexisting molecular and atomic emissions appears from the products of plasma generation process. At low pressure, the interference of the continuum emission from plasma itself decreases dramatically. Because the collisional and plasma quenching processes are not significant under reduced pressure conditions, stable and longer existing plasma is formed through the plasma expansion, which makes the signal detection much easier with low interference.

Another important strategy of this study is the control of the electron impact ionization process by the laser pulse width. Once charged particles are produced by multi-photon ionization, laser energy will be absorbed by the inverse bremsstrahlung intensively and plasma grows rapidly by electron impact ionization. This plasma growth process can be controlled using short pulse width lasers, such as picosecond laser. To investigate the phenomena described above, the theoretical model using the lattice Boltzmann method (LBM) was applied and the gas plasma generation processes were analysed using LBM. Maxwell equations, which were used to model the propagation of laser, were calculated by the finite difference time domain (FDTD) method. Employing coefficients of distribution functions, processes of inverse bremsstrahlung, multi-photon ionization, electron impact ionization and three-body recombination were included in Boltzmann equations. Creation and evolution processes of particles (electron, ion, and neutral) in plasma were clarified using LBM to solve the continuous Boltzmann equations used to simulate the generation of plasma. The summery of this theoretical model is described and it is also discussed in detail elsewhere.[29]

LIBS signals arising in plasma cooling period are determined by the initial plasma creation process including multi-photon ionization and electron impact ionization that can be controlled by pressure, laser pulse width, and wavelength. Because the difference of multi-photon ionization rates between N_2 and CH_3I is large and CH_3I is largely dissociated by the laser irradiation,[30] the features of emission signal will also change, which is the study in this paper. At high pressure, electron impact ionization is the major source of plasma generation. Multi-photon ionization becomes the dominant process in plasma generation when reducing the pressure. In this study, low pressure and short pulse laser breakdown was employed to the iodine detection of CH_3I in buffer gases of N_2 and air. The upper level energy of detection species is listed in Table 1.[31] Iodine wavelength at 183 nm (I-3) was the representative signal in this study according to the upper level energy.

Table 1 Upper level energy of detection species

Species	Upper energy (cm^{-1})	Lower energy (cm^{-1})	Wavelength (nm)
I-1	56092.88	0	178.3
I-2	63186.76	7602.97	179.9
I-3	54633.46	0	183
I-4	56092.88	7602.97	206.2
C	61981.82	10192.63	193
N-1	86220.51	28839.31	174.3

Experimental Apparatus

Fig. 1 illustrates the experimental apparatus used in this study. The apparatus fundamentally consisted of lasers, vacuum chamber, lens, detectors and so on. Three different pulse width lasers were employed to measure iodine. Nanosecond laser employed was pulse Nd:YAG laser (Quanta-Ray Pro-230, 6-12 ns, 10 Hz, beam

diameter: 9 mm) operated at fundamental radiation 1064 nm and second harmonic 532 nm with different pulse energy, respectively. The output parameters of picosecond laser 1 (EKSPLA SL312, 150 ps, 10 Hz, beam diameter: 10 mm) were: 1064 nm and 150 mJ/p. The output parameters of picosecond laser 2 (Quantel YG901C-10, 35 ps, 10 Hz, beam diameter: 9.5 mm) were: 1064 nm and 64 mJ/p. The output laser beam was focused into the measurement area using the lens with focal length of 80 mm. The measurement chamber was a vacuum cell with four quartz windows and its internal volume was about 200 cm^3. The path length from the center of chamber to the quartz windows was 65 mm. Perpendicular to laser propagation direction, emission from another window of the chamber was focused onto the spectrometer slit. The focal length of the lens between vacuum chamber and spectrometer was 60 mm. Emission signals were finally detected by combination of a spectrometer (JASCOCT-10S), an ICCD camera (Princeton Instruments Inc., Model ITEA/CCD-576-S/RB-E) and auxiliary equipment. The signal of 100 shots (10 s) was measured three times at each condition. The detection limit was estimated by accumulating signals of 600 shots (1 min). The gate width was set to 30 μs in this study. In the measurement of iodine, the iodine signal was located at vacuum UV region such as 183 nm, in which there was the effect of O_2 absorption. Therefore N_2 was purged along the detection path from the vacuum chamber to the spectrometer, which is shown as the dashed range in Fig. 1.

The standard gas of CH_3I in N_2 with concentration of 101 ppm (Taiyo Nippon Sanso) was used and diluted by the buffer gases of N_2 and air to reduce the concentration around few ppm levels due to the high sensitivity of LIBS technology. The pressure was measured by a pressure gauge (Tem-Tech Lab. SE1000-SNV-420T1) installed at the evacuation port of the chamber.

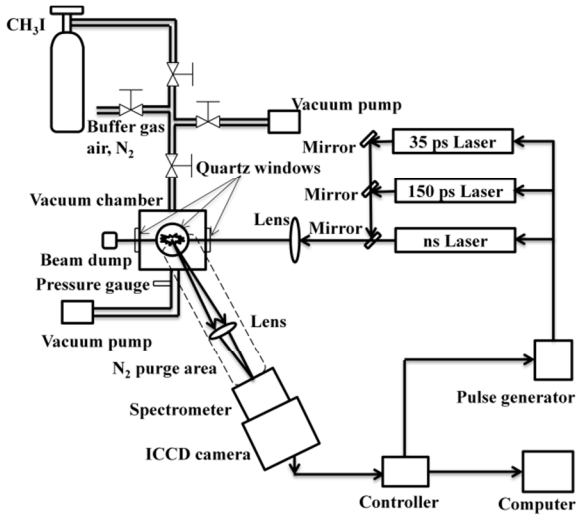

Fig. 1 Schematic diagram of the experimental apparatus

Results and Discussion

There are several interferences with the target signals in LIBS process, generally including the continuum emission from plasma itself, coexisting molecular and atomic emissions, noise from detectors, and so on. Iodine signal in N_2 was measured at the pressure of 30 kPa using ns 1064 nm breakdown. It was difficult to distinguish the signals of iodine and C in short delay time because of the strong interference of the continuum emission from plasma itself. In long delay time of 30 μs and 50 μs, there were discriminable signals of iodine emission, as shown in Fig. 2. In order to confirm the different emission signals, the pure gas of N_2 was also detected under the same conditions, such as N emissions at 174.3 nm (N-1), 184.6 nm, 188.5 nm and 213 nm. The intensity ratio of I-3 to C is much higher in the delay time of 50 μs compared with that in the delay time of 30 μs due to the fact that there is the difference of the upper level energies between C (61981.82 cm^{-1}) and I-3 (54633.46 cm^{-1}). At this range of pressure, the electron impact ionization process becomes the major process to raise the temperature of plasma and the emission signals tended to follow Eq. (1) limiting the improvement of signal to noise ratio.

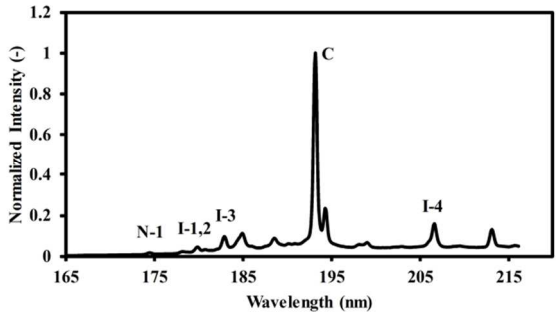

(a) Delay time 30 μs

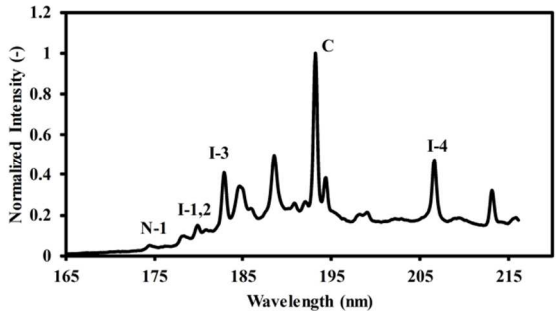

(b) Delay time 50 μs

Fig. 2 LIBS spectra of iodine signal at high pressure. Conditions: ns 1064 nm, power 400 mJ/p, pressure 30 kPa, gate width 30 μs, buffer gas N_2. The signal was normalized by C signal intensity.

Nanosecond breakdown of CH_3I in N_2 under different conditions

Under reduced pressure condition, iodine in buffer gas of N_2 was detected using nanosecond breakdown. Fig. 3 shows the measurement results of iodine signal at low pressure of 1300 Pa using 1064 nm and 532 nm breakdowns with laser power of 400 mJ/p. The obvious iodine signal can be distinguished from the spectra in both cases. These spectra were not detected at 30 kPa by adjusting the delay time. At low pressure, the particles, such as electrons, ions and neutrals, in cold plasma were not in LTE condition. The temperature of plasma mainly referred to the neutrals of excited iodine at low pressure, which was also lower compared with that at higher pressure because of the limited electron impact ionization process. The interference of the continuum emission from plasma itself was reduced when the pressure decreased and iodine emissions became eminent compared with other emission signals. It is also recognized that the iodine emission at 183 nm (I-3) became eminent compared with other emission signals such as N-1 at 174.3 nm using 532 nm breakdown. This effect was also recognized by the laser breakdown time-of-flight mass spectrometry (LB-TOFMS) and it was observed that 532 nm can dissociate CH_3I much more efficiently compared to N_2.[30] It is also worth noting that the lower electron density produced by 532 nm breakdown reduced

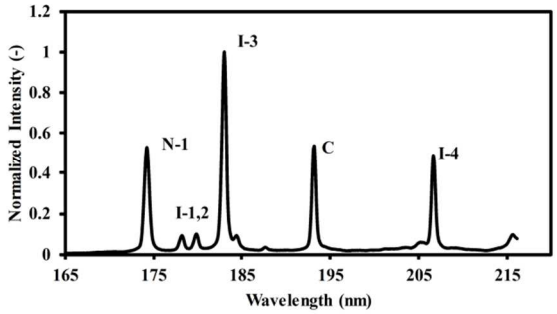

(a) ns 1064 nm breakdown

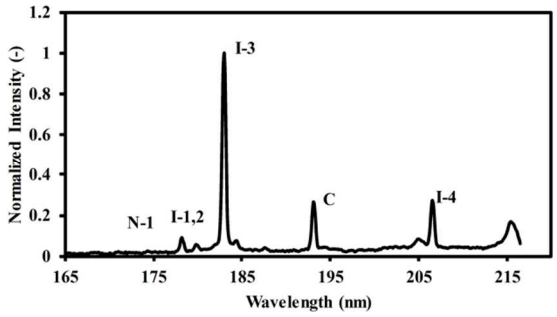

(b) ns 532 nm breakdown

Fig. 3 LIBS spectra of iodine signal at low pressure using nanosecond breakdown. Conditions: power 400 mJ/p, pressure 1300 Pa, delay time 1060 ns, gate width 30 μs, buffer gas N_2. The signal was normalized by iodine signal of I-3.

the effect of electron impact ionization because of the lower efficiency of inverse bremsstrahlung process, which is approximately proportional to wavelength square.[32]

Employing ns 1064 nm breakdown with laser power of 400 mJ/p and 1000 mJ/p, iodine signal was measured under different pressure and delay time conditions. Nanosecond laser operated at 532 nm with power of 400 mJ/p was also employed to measure iodine under different conditions. When the pressure decreased, the effect of electron impact ionization can be reduced. As N_2 was the buffer gas, N emission at 174.3 nm (N-1) was determined as the coexisting atomic emissions to clarify the plasma generation process including the multi-photon ionization and electron impact ionization processes. Iodine emission at 183 nm (I-3) was set as a representative signal. Compared with the iodine signal at 183 nm (I-3), the N signal was mainly produced by the electron impact ionization process due to the higher upper level energy of N-1 emission. The intensity ratio of I-3 at 183 nm to N-1 at 174.3 nm was chosen to compare the breakdown characteristics.

Figs. 4(a), 4(b) and 4(c) show the delay time dependence of I_{I-3}/I_{N-1} under different conditions. When the pressure reduced at low pressure area (less than 3000 Pa), the intensity ratio of I-3 to N-1 increased, which also demonstrated the satisfied results using low pressure LIBS. The intensity ratio of I-3 to N-1 also increased with an increase in delay time due to the lower upper level energy of iodine compared with that of N, as shown in Table 1.

Comparing the results using 1064 nm breakdown at different power, the intensity ratio of I-3 to N-1 using 400 mJ/p was better than that using 1000 mJ/p, as Fig. 4(a) and Fig. 4(b) show. The increased laser power strengthened the electron impact ionization process, which resulted in the significant increase of N signal intensity. In the case of ns 532 nm

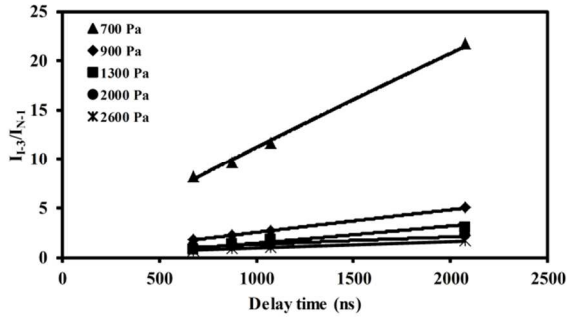

(a) Delay time dependence of I_{I-3}/I_{N-1} using ns 1064 nm breakdown at 400 mJ/p

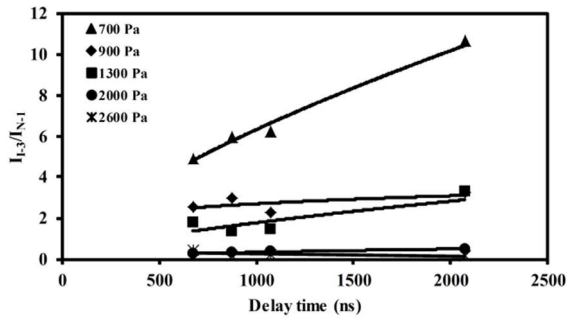

(b) Delay time dependence of I_{I-3}/I_{N-1} using ns 1064 nm breakdown at 1000 mJ/p

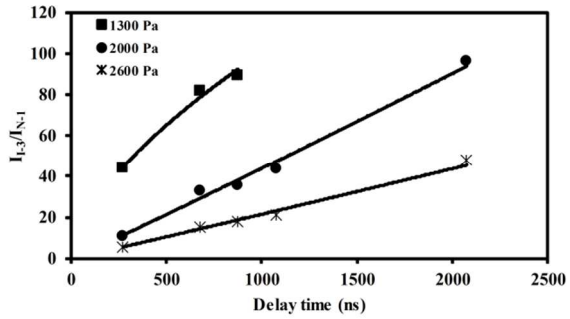

(c) Delay time dependence of I_{I-3}/I_{N-1} using ns 532 nm breakdown at 400 mJ/p

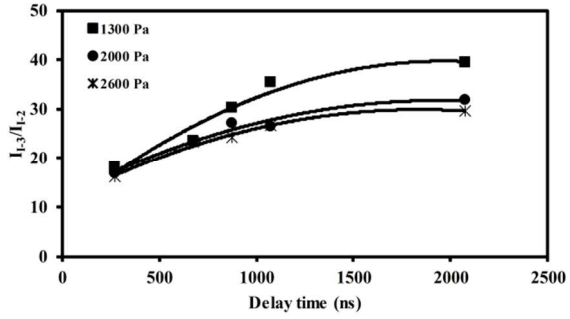

(d) Delay time dependence of I_{I-3}/I_{I-2} using ns 532 nm breakdown at 400 mJ/p

Fig. 4 Delay time dependence of iodine signal at different pressure. Conditions: gate width 30 μs, buffer gas N_2.

breakdown, at low pressure of 700 Pa and 900 Pa, there was clear I-3 signal without N-1 signal at 174.3 nm because of the larger ionization and excitation processes. Compared Fig. 4(a)

with Fig. 4(c), the intensity ratio of I-3 to N-1 was much higher in the case of 532 nm breakdown. This was occurred because of the different photon energy leading to the dissociation of CH_3I. The photon energy of 532 nm is double compared with that of 1064 nm. Employing 532 nm breakdown, the multi-photon ionization process is much more efficient due to the higher photon energy,[33] leading to the eminent iodine signal intensity at the same condition. Another reason was the efficient electron impact ionization by 1064 nm, resulting in the increase of signal intensity especially the N signal. All these two causes led to the higher intensity ratio of I-3 to N-1 using 532 nm breakdown.

As is known from these results, the plasma temperature reduced when the pressure decreased because the effect of electron impact ionization was reduced in these three cases. The intensity ratio of I-3 to N-1 increased at reduced pressure. Especially the large increase appeared at the lower pressure, such as 700 Pa using 1064 nm breakdown and 1300 Pa using 532 nm breakdown. The finding was explained by the comparison of delay time dependence of I_{I-3}/I_{N-1} and I_{I-3}/I_{I-2} at different pressure, as shown in Fig. 4(c) and Fig. 4(d). The intensity ratio of the emission pair of iodine atom can be used as an indicator of iodine temperature. Among iodine emission lines I_{I-3}/I_{I-2} was used as this indicator in this study, because there is enough difference of the upper level energies between I-2 and I-3. It is also mentioned that despite the upper level energy of I-4, the behavior of I-4 showed almost the same tendency as that of I-2 and I-4 is not suitable as an indicator in this study. We assume that there is a mixing of different emission lines at 206.2 nm or other effects such as resonant phenomena.

The increase of I_{I-3}/I_{I-2} means the decrease of temperature. These results confirmed the decrease of temperature with the increase of delay time and decrease of pressure. The difference of I_{I-3}/I_{I-2} between each presssure in same delay time was not similar to that of I_{I-3}/I_{N-1}. Therefore, the decrease of plasma temperature was not the only cause to increase the intensity ratio of I-3 to N-1 at reduced pressure and the discrepancy from the LTE condition at reduced pressure produced more population of iodine at excited levels. Even more important, the iodine can be ionized and excited largely at low pressure compared with the coexisting atom of N. The consistent results can also be clarified in the cases of ns 1064 nm breakdown. However, the more significant larger ionization and excitation appeared when using 532 nm breakdown.

Picosecond breakdown of CH_3I in N_2 under different conditions

The laser-induced plasma process can be controlled by pressure and laser pulse width. Short pulse laser irradiation allowed for a specificity of excitation that could yield LIBS signals more tightly correlated to particular chemical species and showed significantly lower background emission. Short pulse lasers with pulse widths of 150 ps and 35 ps were employed to discuss the plasma generation process. Fig. 5 shows the measurement results of iodine emissions in N_2 using 150 ps and 35 ps lasers operated at 1064 nm, which indicates that the signal of I-3 was the main spectral line. Compared with Fig. 3(a), the iodine signal (I-3) became clearer using short pulse width breakdown. The coexisting atom emissions and the continuum emission from plasma itself were reduced when employing short pulse breakdown, especially 35 ps breakdown.

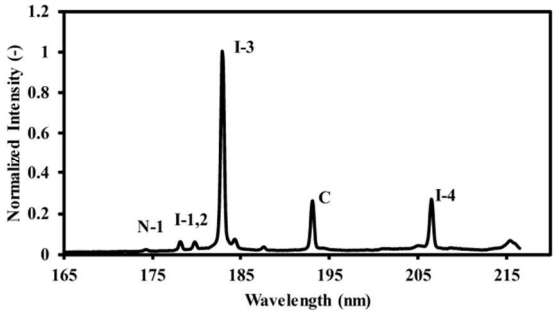

(a) 150 ps 1064 nm breakdown

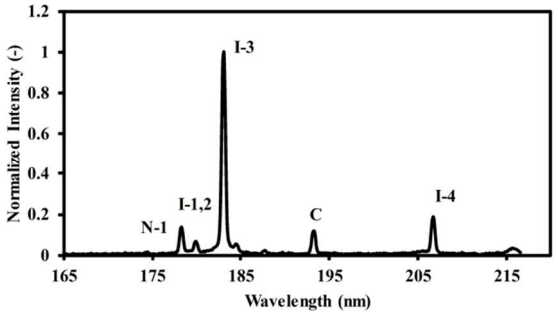

(b) 35 ps 1064 nm breakdown

Fig. 5 LIBS spectra of iodine signal at low pressure using picosecond breakdown. Conditions: 150 ps laser at 1064 nm with power 150 mJ/p, 35 ps laser at 1064 nm with power 64 mJ/p, pressure 1300 Pa, delay time 1060 ns, gate width 30 μs, buffer gas N_2. The signal was normalized by iodine signal of I-3.

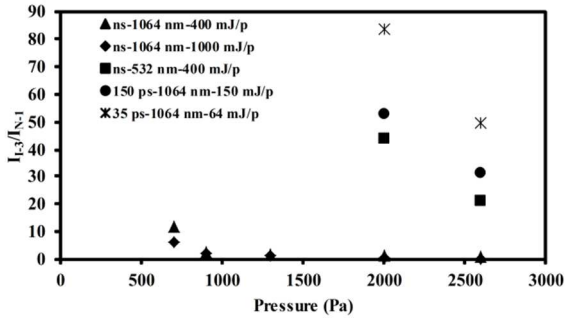

Fig. 6 Pressure dependence of I_{I-3}/I_{N-1} in N_2. Conditions: delay time 1060 ns, gate width 30 μs.

Under different pressure and delay time conditions, iodine signal was detected using these two short pulse width lasers. Fig. 6 shows the pressure dependence of I_{I-3}/I_{N-1} under different breakdown conditions. When reducing the pressure, the intensity ratio of I-3 to N-1 increased in all cases. Short pulse width and short wavelength breakdown performed the improved intensity ratio of I-3 to N-1. Nanosecond breakdown at different power and wavelength has been already discussed in the previous section. Taking all the conditions into consideration, the reasons for the improved results were the control of the laser-induced plasma process, especially electron impact ionization process, and the larger ionization and excitation of iodine. The coexisting molecular and atomic emissions usually appear during the electron impact ionization process. The interference of coexisting atomic emission, i.e. N

emission, was diminished employing short pulse width and short wavelength breakdown.

Detection limit of iodine in buffer gases of N_2 and air

Fig. 7 shows the concentration dependence of iodine signal intensity in buffer gas of N_2 using ns 1064 nm, ns 532 nm and 35 ps 1064 nm breakdowns. The results suggest the linear growth of the intensity of I-3 signal.

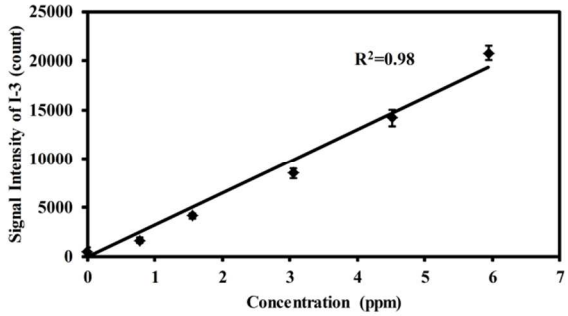

(a) ns 1064 nm breakdown

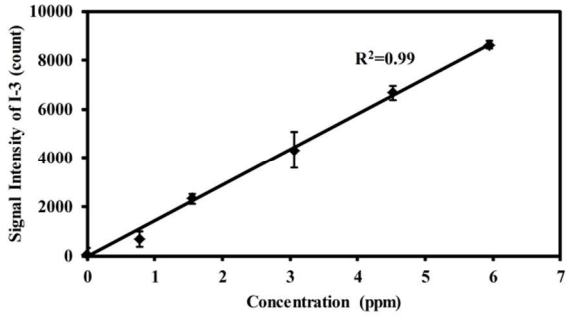

(b) ns 532 nm breakdown

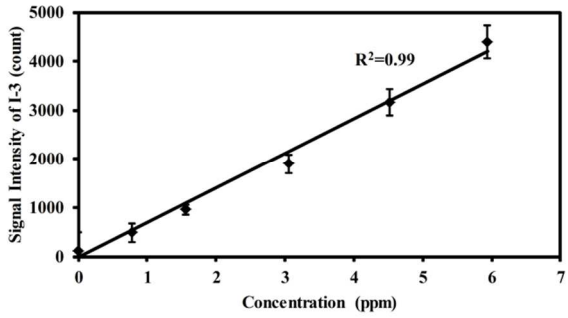

(c) 35 ps 1064 nm breakdown

Fig. 7 Concentration dependence of iodine signal intensity in N_2. (a) ns 1064 nm breakdown. Conditions: power 400 mJ/p, pressure 700 Pa, delay time 1060 ns. (b) ns 532 nm breakdown. Conditions: power 400 mJ/p, pressure 1300 Pa, delay time 260 ns. (c) 35 ps 1064 nm breakdown. Conditions: power 64 mJ/p, pressure 1300 Pa, delay time 260 ns. Gate width 30 μs, buffer gas N_2. The error bar was denoted using the standard deviation of three times measurements.

Iodine was also measured in buffer gas of air to evaluate the buffer gas effect at reduced pressure conditions. Fig. 8 shows the measurement results of iodine in air at 700 Pa using nanosecond and 35 picosecond lasers operated at 1064 nm. O_2 absorption around 183 nm was not significant at such low pressure of 700 Pa inside the chamber because the absorption cross section of O_2 at 183 nm is around 10^{-21} cm^2 [34] and its effect is less than 1% according to the Beer-Lambert law. The LIBS spectra in buffer gas of air were different from that in buffer gas of N_2 because of the reduction of iodine signal by the effect of oxygen. The iodine signal (I-3) at 183 nm was reduced markedly due to the high quenching rate of excited iodine in buffer gas of air. According to the comparison of Fig. 8(a) and Fig. 8(b), the continuum emission from plasma itself was reduced when employing 35 ps breakdown, which led to the increase of signal to background ratio in the case of short pulse laser breakdown. These measurement results were consistent with those in buffer gas of N_2.

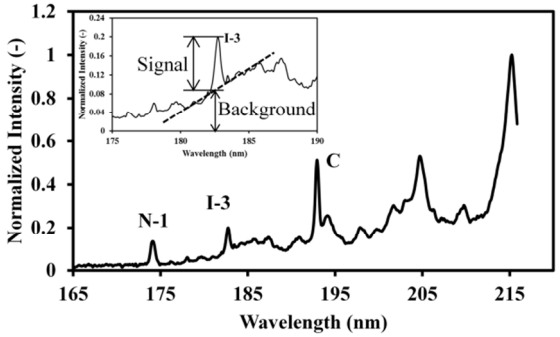

(a) ns 1064 nm breakdown

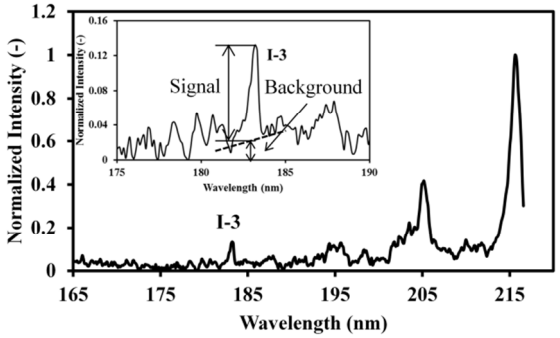

(b) 35 ps 1064 nm breakdown

Fig. 8 LIBS spectra of iodine signal in air. (a) ns 1064 nm breakdown. Conditions: power 1000 mJ/p, pressure 700 Pa, delay time 260 ns, gate width 30 μs, CH_3I 500 ml/min, air 2.0 l/min. (b) 35 ps 1064 nm breakdown. Conditions: power 64 mJ/p, pressure 700 Pa, delay time 60 ns, gate width 30 μs, CH_3I 500 ml/min, air 2.0 l/min. The signal was normalized by the maximum.

According the measurement results, the detection limit can be enhanced using low pressure LIBS. As for the measurement of iodine in N_2 at low pressure, the iodine detection limit of 600 shots (1 min) in buffer gas of N_2 was estimated by evaluating the ratio of the slope of the iodine signal calibration curve (m_s) to the background noise (standard deviation: σ). The iodine detection limit was 60 ppb ($3\sigma/m_s$) in nanosecond breakdown at pressure of 700 Pa. The background emission around I-3 at 183 nm was not eminent and the iodine detection limit was mainly determined by the detector noise in buffer gas of N_2. Therefore, there was not evident enhancement of iodine detection limit employing short pulse width breakdowns. The detection limit of iodine in air became worse due to the high quenching rate of excited iodine in buffer gas of air.

Conclusion

This study focused on the trace species of iodine measurement. Iodine in buffer gases of N_2 and air was measured using low pressure LIBS under different experimental conditions, i.e.

pressure, delay time, pulse width, buffer gas etc. when employing standard gas of CH_3I to detect iodine signal.

1) Under low pressure conditions, the obvious iodine signals, especially I-3 at 183 nm, were distinguished compared with that at higher pressure. The interference of the continuum emission from plasma itself reduced when the pressure decreased.

2) Nanosecond laser was employed to measure iodine signal under different pressure and delay time conditions. The intensity ratio of I-3 to N-1 was improved when reducing the pressure and increasing the delay time. Low laser power at 1064 nm breakdown and short wavelength of 532 nm breakdown performed the improved intensity ratio of I-3 to N-1 due to the control of the electron impact ionization process and the efficiently larger ionization and excitation of iodine.

3) The plasma generation process was controlled by the pulse width except for the pressure. Short pulse width lasers including 150 ps and 35 ps lasers were employed to measure iodine signal. The intensity ratio of I-3 to N-1 was enhanced using short pulse width lasers, especially 35 ps laser.

4) The spectra in air were different from that in N_2 due to the high quenching rate of excited iodine in buffer gas of air. Using low pressure LIBS, it is feasible to measure iodine in air, especially short pulse laser breakdown. The detection limit of iodine in N_2 was 60 ppb ($3\sigma/m_s$) in nanosecond breakdown at pressure of 700 Pa.

Notes and references

[a] State Key Laboratory of Multiphase Flow in Power Engineering, Xi'an Jiaotong University, Xi'an 710049, China

[b] Graduate School of Advanced Technology and Science, The University of Tokushima, Tokushima 770-8501, Japan

1 S. Mishra, V. Singh, A. Jain and K.K. Verma, Determination of iodide by derivatization to 4-iodo-N,N-dimethylaniline and gas chromatography–mass spectrometry. *Analyst*, 2000, **125**, 459.

2 P. Das, M. Gupta, A. Jain and K.K. Verma, Single drop microextraction or solid phase microextraction–gas chromatography–mass spectrometry for the determination of iodine in pharmaceuticals, iodized salt, milk powder and vegetables involving conversion into 4-iodo-N,N-dimethylaniline. *J. Chromatogr., A*, 2004, **1023**, 33.

3 S. Zhang, K.A. Schwehr, Y.-F. Ho, C. Xu, K.A. Roberts, D.I. Kaplan, R. Brinkmeyer, C.M. Yeager, and P.H. Santschi, A novel approach for the simultaneous determination of iodide, iodate and organo-iodide for ^{127}I and ^{129}I in environmental samples using gas chromatography-mass spectrometry. *Environ. Sci. Technol.*, 2010, **44**, 9042.

4 R.J. Huang, X. Hou and T. Hoffmann, Extensive evaluation of a diffusion denuder technique for the quantification of atmospheric stable and radioactive molecular iodine. *Environ. Sci. Technol.*, 2010, **44**, 5061.

5 Ph. Bienvenu, E. Brochard, E. Excoffier and M. Piccione, Determination of iodine 129 by ICP-QMS in environmental samples. *Can. J. Anal. Sci. Spectrosc*., 2004, **49**, 423.

6 T. Nakahara and T. Mori. Analyte Volatilization Procedure for the determination of low concentrations of iodine by inductively coupled plasma atomic emission spectrometry. *J. Anal. At. Spectrom.*, 1994, **9**,159.

7 A.A. Oliveira, L.C. Trevizan and J.A. Nóbrega, Review: iodine determination by inductively coupled plasma spectrometry. *Appl. Spectrosc. Rev.*, 2010, **45**, 447.

8 P. Grinberg and R.E. Sturgeon, Ultra-trace determination of iodine in sediments and biological material using UV photochemical generation-inductively coupled plasma mass spectrometry. *Spectrochim. Acta Part B*, 2009, **64**, 235.

9 D.A. Cremers and L.J. Radziemski, Detection of chlorine and fluorine in air by laser-induced breakdown spectrometry. *Anal. Chem.*, 1983, **55**, 1252.

10 L.J. Radziemski, T.R. Loree, D.A. Cremers and N.M. Hoffman, Time-resolved laser-induced breakdown spectrometry of aerosols. *Anal. Chem.*, 1983, **55**, 1246.

11 Z.Z. Wang, Y. Deguchi, M. Kuwahara, J.J. Yan and J.P. Liu, Enhancement of laser-induced breakdown spectroscopy (LIBS) detection limit using a low-pressure and short-pulse laser-induced plasma process. *Appl. Spectrosc*., 2013, **67**, 1242.

12 Z.Z. Wang, Y. Deguchi, M. Kuwahara, T. Taira, X.B. Zhang, J.J. Yan, J.P. Liu, H. Watanabe and R. Kurose, Quantitative elemental detection of size-segregated particles using laser-induced breakdown spectroscopy. *Spectrochim. Acta Part B*, 2013, **87**, 130.

13 F.R. Doucet, G. Lithgow, R. Kosierb, P. Bouchard and M. Sabsabi, Determination of isotope ratios using laser-induced breakdown spectroscopy in ambient air at atmospheric pressure for nuclear forensics. *J. Anal. At. Spectrom.*, 2011, **26**, 536.

14 M. Noda, Y. Deguchi, S. Iwasaki and N. Yoshikawa, Detection of carbon content in a high-temperature and high-pressure environment using laser-induced breakdown spectroscopy. *Spectrochim. Acta Part B*, 2002, **57**, 701.

15 M. Kurihara, K. Ikeda, Y. Izawa, Y. Deguchi and H. Tarui, Optimal boiler control through real-time monitoring of unburned carbon in fly ash by laser-induced breakdown spectroscopy. *Appl. Opt*. 2003, **42**, 6159.

16 D.A. Cremers, L.J. Radziemski and T.R. Loree, Spectrochemical analysis of liquids using the laser spark. *Appl. Spectrosc*., 1984, **38**, 721.

17 R.W. Joseph and A.C. David, Determination of uranium in solution using laser-induced breakdown spectroscopy. *Appl. Spectrosc*., 1987, **41**, 1042.

18 H. Loudyi, K. Rifaï, S. Laville, F. Vidal, M. Chaker and M. Sabsabi, Improving laser-induced breakdown spectroscopy (LIBS) performance for iron and lead determination in aqueous solutions with laser-induced fluorescence (LIF). *J. Anal. At. Spectrom.*, 2009, **24**, 1421.

19 M. Gaft, I. Sapir-Sofer, H. Modiano and R. Stana, Laser induced breakdown spectroscopy for bulk minerals online analyses. *Spectrochim. Acta Part B*, 2007, **62**, 1496.

20 J.L. Gottfried, R.S. Harmon, F.C. De Lucia Jr. and A.W. Miziolek, Multivariate analysis of laser-induced breakdown spectroscopy chemical signatures for geomaterial classification. *Spectrochim. Acta Part B*, 2009, **64**, 1009.

21 J.L. Gottfried, F.C. De Lucia Jr. and A.W. Miziolek, Discrimination of explosive residues on organic and inorganic substrates using laser-induced breakdown spectroscopy. *J. Anal. At. Spectrom.*, 2009, **24**, 288.

22 T.B. Yuan, Z. Wang, L.Z. Li, Z.Y. Hou, Z. Li and W.D. Ni, Quantitative carbon measurement in anthracite using laser-induced breakdown spectroscopy with binder. *Appl. Optics*, 2012, **51**, B22.

23 T.B. Yuan, Z. Wang, S.L. Lui, Y.T. Fu, Z. Li, J.M. Liu and W.D. Ni, Coal property analysis using laser-induced breakdown spectroscopy. *J. Anal. At. Spectrom.*, 2013, **28**, 1045.

24 J.S. Xiu, V. Motto-Ros, G. Panczer, R. Zheng and J. Yu, Feasibility of wear metal analysis in oils with parts per million and sub-parts per million sensitivities using laser-induced breakdown spectroscopy of thin oil layer on metallic target. *Spectrochim. Acta Part B*, 2014, **91**, 24.

25 R.L.H. Megan, M. Joseph, O. Robert, B. Jennifer, D. Yamac, M. Caroline and B.S. James, Ultrafast laser-based spectroscopy and sensing: applications in LIBS, CARS, and THz spectroscopy. *Sensors*, 2010, **10**, 4342.

26 K.L. Eland, D.N. Stratis, T. Lai, M.A. Berg, S.R. Goode and S.M. Angel, Some comparisons of LIBS measurements using nanosecond and picosecond laser pulses. *Appl. Spectrosc*., 2001, **55**, 279.

27 Y. Deguchi, *Industrial Applications of Laser Diagnostics*. ed. CRC Press, New York, 2011.

28 G. Cristoforetti, E. Tognoni and L.A. Gizzi, Thermodynamic equilibrium states in laser-induced plasmas: From the general case to laser-induced breakdown spectroscopy plasmas. *Spectrochim. Acta Part B*, 2013, **90**, 1.

29 X.B. Zhang, Y. Deguchi and J.P. Liu, Numerical simulation of laser induced weakly ionized helium plasma process by lattice Boltzmann method. *Jpn. J. Appl. Phys*., 2012, **51**, 01AA04.

30 Z.Z. Wang, Y. Deguchi, J.J. Yan and J.P. Liu, Rapid detection of mercury and iodine using laser breakdown time-of-flight mass spectrometry. Spectrosc. Lett., 2014, DOI: 10.1080/00387010.2013.859158.

31 A. Kramida, Yu. Ralchenko, J. Reader, and NIST ASD Team (2013). NIST Atomic Spectra Database (ver. 5.1), [Online]. Available: http://physics.nist.gov/asd. National Institute of Standards and Technology, Gaithersburg, MD. 2014.

32 L.M. Cabalin and J.J. Laserna, Experimental determination of laser induced breakdown thresholds of metals under nanosecond Q-switched laser operation. *Spectrochim. Acta Part B*, 1998, **53**, 723.

33 D. M. Lubman, *Lasers and Mass Spectrometry*. Oxford University Press, Oxfored, 1990.

34 M. Ogawa, Absorption cross sections of O_2 and CO_2 continua in the schumann and far-uv regions. The Journal of Chemical Physics 1971, **54**, 2550.

Iodine in buffer gases of air and N_2 was measured under various conditions including different wavelength, laser power, pulse width and pressure to compare the detection characteristics of low pressure and short pulse LIBS.